

Research Article

Network Pharmacology-Based Prediction of the Active Compounds, Potential Targets, and Signaling Pathways Involved in Danshiliuhao Granule for Treatment of Liver Fibrosis

Yueying Tao ^{1,2}, Kunming Tian,³ Ji Chen,⁴ Danfeng Tan,² Yan Liu,⁵
Yongai Xiong,² Zehui Chen ¹ and Yingbiao Tian ^{1,2}

¹The Affiliated Hospital of Zunyi Medical University, Zunyi 563000, China

²School of Pharmacy, Zunyi Medical University, Zunyi 563003, China

³Department of Preventive Medicine, School of Public Health, Zunyi Medical University, Zunyi 563003, China

⁴Department of Pharmacy, Zunyi Second People's Hospital, Zunyi 563000, China

⁵The Second Affiliated Hospital of Zunyi Medical University, Zunyi 563003, China

Correspondence should be addressed to Zehui Chen; 941291773@qq.com and Yingbiao Tian; tybczh@163.com

Received 3 April 2019; Revised 13 May 2019; Accepted 22 May 2019; Published 3 July 2019

Academic Editor: Ferdinando Nicoletti

Copyright © 2019 Yueying Tao et al. This is an open access article distributed under the Creative Commons Attribution License, which permits unrestricted use, distribution, and reproduction in any medium, provided the original work is properly cited.

This study aims to predict the active ingredients, potential targets, signaling pathways and investigate the “ingredient-target-pathway” mechanisms involved in the pharmacological action of Danshiliuhao Granule (DSLHG) on liver fibrosis. Pharmacodynamics studies on rats with liver fibrosis showed that DSLHG generated an obvious anti-liver fibrosis action. On this basis, we explored the possible mechanisms underlying its antifibrosis effect using network pharmacology approach. Information about compounds of herbs in DSLHG was collected from TCMSP public database and literature. Furthermore, the oral bioavailability (OB) and drug-likeness (DL) were screened according to ADME features. Compounds with $OB \geq 30\%$ and $DL \geq 0.18$ were selected as active ingredients. Then, the potential targets of the active compounds were predicted by pharmacophore mapping approach and mapped with the target genes of the specific disease. The compound-target network and Protein-Protein Interaction (PPI) network were built by Cytoscape software. The core targets were selected by degree values. Furthermore, GO biological process analysis and KEGG pathway enrichment analysis were carried out to investigate the possible mechanisms involved in the anti-hepatic fibrosis effect of DSLHG. The predicted results showed that there were 108 main active components in the DSLHG formula. Moreover, there were 192 potential targets regulated by DSLHG, of which 86 were related to liver fibrosis, including AKT1, EGFR, and IGF1R. Mechanistically, the anti-liver fibrosis effect of DSLHG was exerted by interfering with 47 signaling pathways, such as PI3K-Akt, FoxO signaling pathway, and Ras signaling pathway. Network analysis showed that DSLHG could generate the antifibrosis action by affecting multiple targets and multiple pathways, which reflects the multicomponent, multitarget, and multichannel characteristics of traditional Chinese medicine and provides novel basis to clarify the mechanisms of anti-liver fibrosis of DSLHG.

1. Introduction

Liver fibrosis is a common pathological feature of chronic liver disease and a main contributor in the development of cirrhosis caused by chronic liver injury [1, 2]. It is characterized by excessive deposition of collagen-based extracellular matrix (ECM) in the liver and abnormal liver function. Various chemical/microbial factors could contribute to the occurrence of hepatic fibrosis, including alcohol, virus, drugs,

toxicants, and autoimmune process [3–6]. Previous studies [7, 8] indicated that liver fibrosis, especially in early stage, could be reversed, while once the liver fibrosis develops into cirrhosis stage, it could not. Thereby, more and more scholars are working to find novel drugs that can effectively reverse or delay the development of hepatic fibrosis.

Since the 1970s, the traditional Chinese medicine (TCM) have been used for the treatment of liver fibrosis. Cumulating data have shown that the TCM compound possesses

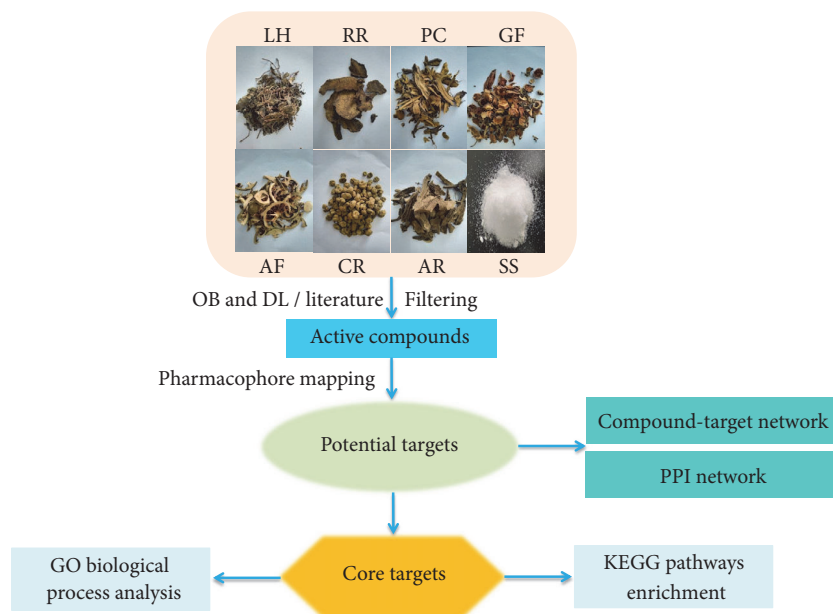


FIGURE 1: The schematic illustration of network pharmacology analysis.

obvious advantages in treatment of liver fibrosis. However, due to the multicomponent, multitarget, and multichannel characteristics of TCM and their complex formulations, the detailed medicinal ingredients of Chinese medicines and their complex models of action are unclear, which impeded the modernization and clinical application of TCM [9–11]. In recent years, network pharmacology based on systems biology and polypharmacology is emerging. Network pharmacology explores the relevance of drug-disease from a holistic and systematic perspective, emphasizes the transition of research mode from “single target” to “multiple targets,” and systematically expounds the principles and rules of interaction between organism and drugs. As a powerful tool for exploring the potential mechanisms of various actions of TCM formulas and novel active ingredients via constructing a network of interactions between drugs and genes, targets and diseases, it has been widely used in TCM research and became a new approach for the development of TCM [10–12].

Danshiliuhao Granule (DSLHG, composed of *Lysimachiae Herba* (LH), *Polygoni Cuspidati Rhizoma Et Radix* (PC), *Radix et Rhizoma Rhei* (RR), *Gardeniae Fructus* (GF), *Aurantii Fructus* (AF), *Aucklandiae Radix* (AR), *Corydalis Rhizoma* (CR), and Sodium Sulfate (SS)) is a Chinese herb preparation based on TCM prescription with wonderful anti-liver fibrosis effect and preservation of liver function. Our work provided theoretical basis for the registration of pharmaceutical preparations and laid the foundation for the subsequent acquisition of new medicine certificates. Among these herbal medicines, RR is a commonly used TCM. Many studies have proven that emodin has good clinical value in the treatment of liver fibrosis [13–15]. The rhein possesses anti-inflammatory and free radical scavenging effects and antifibrosis effect, protects liver cells, and reduces liver damage [16]. Additionally, PC exerts antibacterial, antiviral, and

liver protection effect that can promote liver cell regeneration and recovery. Thereby, the beneficial effects of PC make it have therapeutic effect on acute hepatic ischemic injury, as evidenced by abrogated acute liver injury caused by carbon tetrachloride (CCl_4) [17, 18]. In our study, we found that DSLHG could alleviate liver fibrosis induced by CCl_4 in rats and raised one new hopeful drug for the treatment of hepatic fibrosis. However, due to its complex components and molecular mechanisms against liver fibrosis, which have not been fully elucidated, it is of great significance to explore the anti-liver fibrosis mechanisms of DSLHG through network pharmacology.

In this work, we investigated the pharmacological mechanisms by which DSLHG regulates liver fibrosis. For this purpose, we established and analyzed active compound-target (C-T) network. First of all, we selected the active ingredients according to pharmacokinetic parameters (oral bioavailability and drug-likeness) from public database and searched the potential targets of these compounds by PharmMapper server. Furthermore, we built a network of interactions among active components regarding their related-targets and target genes of liver fibrosis. Moreover, we conducted GO function analysis and relevant pathway enrichment analysis for the potential core targets of DSLHG acting on targeted disease. The schematic illustration of this study is shown in Figure 1.

2. Materials and Methods

2.1. Reagents and Chemicals. Silibinin capsules were provided by Tianjin TASLY SANTS Pharmaceutical CO., Ltd. (Tianjin, China). CCl_4 was obtained from Shanghai Aladdin Bio-Chem Technology Co., Ltd. (Shanghai, China). Olive oil was purchased from Shanghai Yien Chemical Technology

Co., Ltd. (Shanghai, China). CCl_4 was diluted to 40% (v/v) with olive oil before being used. The detection kits of alanine aminotransferase (ALT), aspartate aminotransferase (AST), alkaline phosphatase (ALP), and albumin (ALB) were purchased from the Nanjing Jiancheng Bioengineering Institute (Nanjing, China). Enzyme-linked immunosorbent assay (ELISA) kits for the measurement of laminin (LN), hyaluronic acid (HA), procollagen-III-peptide (PIIINP), and collagen type IV (Col IV) were offered by Shanghai Jiang Lai Biological Technology Co., Ltd. (Shanghai, China).

2.2. Animals and Experimental Design. Sixty healthy male Sprague Dawley (SD) rats weighting 180-220 g were purchased from the Changsha Tianqin Biotechnology Co., Ltd. (Changsha, China). All the animals were housed under the same controlled conditions with a 12 h light-dark cycle at $23\pm 2^\circ\text{C}$ temperature in the Laboratory Animal Center of Zunyi Medical University (Guizhou, China). Then, the rats were randomly divided into 6 groups with 10 rats in each group: named (I): normal control group, (II): model group, (III): positive control group (Silibinin $36\text{ mg/kg}\cdot\text{d}^{-1}$), (IV): DSLHG high-dose group ($27\text{ g/kg}\cdot\text{d}^{-1}$), (V): DSLHG medium-dose group ($13.5\text{ g/kg}\cdot\text{d}^{-1}$), (VI): DSLHG low-dose group ($6.75\text{ g/kg}\cdot\text{d}^{-1}$). All groups were given normal water and standard rat feed. From the first day of the experiment, the abdominal cavities of other rats were injected 40% CCl_4 with olive oil (0.2 mL per 100 g of bodyweight) twice a week (Tuesday and Friday) except for the normal control group, and the normal rats were handled by intraperitoneal injection with olive oil solution (2 mL/kg) for seven weeks. From the 2th week, the positive control group was intragastrically administered with a dose of 10 mL/kg body weight of silibinin, and the DSLHG groups were gavaged with 10 mL/kg body weight of the corresponding drug concentration. In addition, the normal control group and the model group were given a gavage of distilled water of the same volume with the drug. Administration of all animals was continued for six weeks.

At the end of the eighth week, all rats were anesthetized by ether after the last gavage. Then, blood samples were collected from the rat eyelid by capillary. The whole blood was centrifuged at 3500 rpm for 10 min, and the upper serum was taken in a cryogenic vial and then immediately stored in a refrigerator at -20°C to test related biochemical indicators using corresponding kits. The liver tissues of the rats were removed rapidly and rinsed in pre-cold physiological saline. The right lobes of the liver (approximately $1\times 1\text{cm}^3$) were quickly fixed in 10% neutral formaldehyde solution for histopathological examination.

This protocol was approved by the Animal Care and Use Committee of the Zunyi Medical University (2019A-002) and all experimental procedures were in compliance with the National Institutes of Health Guide for Care and Use of Laboratory Animals.

2.3. Histopathological Examination. The fixed liver tissues with 10% neutral buffered formaldehyde solution were dehydrated by automatic dehydrator, embedded in paraffin, and

then sliced to a thickness of 4-6 μm sections. Hematoxylin-eosin (H&E) staining and Masson's trichrome staining were performed to observe the pathological and fibrosis changes, respectively. The degree of inflammation was graded based on the METAVIR scoring system: A0: no activity; A1: mild activity; A2: moderate activity; A3: severe activity. The degree of liver fibrosis was graded on a 5-point scale as either F0, F1, F2, F3, or F4, i.e., no fibrosis, portal fibrosis without septa, portal fibrosis with few septa, numerous septa without cirrhosis, and cirrhosis.

2.4. Chemical Ingredients Database Construction. Information of chemical compounds of each herbal medicine in DSLHG was obtained from free public database and literature. Traditional Chinese Medicine Systems Pharmacology Database and Analysis Platform [19] (TCMSP, <http://lsp.nwu.edu.cn/tcmsp.php>), a unique system pharmacology platform designed for herbal medicines, provides a chemical screening process based on ADME features. According to the pharmacokinetic characteristics given by the TCMSP data platform, the chemical components that cannot satisfy both oral bioavailability (OB) $\geq 30\%$ and drug-likeness (DL) ≥ 0.18 are deleted [20]. The 2D structure of the candidate compound was searched by the PubChem database and drew with ChemBioDraw 14.0 software. Finally, the 2D structure was converted to 3D structure and saved as a MOL2 file.

2.5. Target Genes Related to the Identified Compounds. The target prediction for the main active compounds was performed using the PharmMapper server [21] (<http://www.lilab.ecust.cn/pharmmapper/>) with the "Homo sapiens" species setting, which is a free public web-server that uses active small molecules as a probe to search potential drug targets. The 10 targets with the highest Fit Score were selected, and gene information including gene ID, name, and organism was identified using UniProt database (<https://www.uniprot.org/>).

2.6. Potential Target Genes for Liver Fibrosis. The target genes associated with hepatic fibrosis were collected from the following resources: (1) GeneCards [22] (<https://www.genecards.org/>) is a human gene database that automatically integrates data from approximately 150 web sources. We searched GeneCards database with the keywords "hepatic fibrosis" or "liver fibrosis" and found 1,222 genes related to hepatic fibrosis from the database. (2) The Online Mendelian Inheritance in Man (OMIM) database [23] is a continuously updated database of human genes and genetic disorders. We retrieved 50 hepatic fibrosis-related genes from the OMIM database. (3) Literature, we gathered liver fibrosis-related literature that contains 81 target genes. We finally collected a total of 1,280 genes associated with liver fibrosis through the above sources.

2.7. Construction of Network. In order to understand the mechanisms of DSLHG for the treatment of liver fibrosis, network analysis was performed. The corresponding network was established and visualized by Cytoscape 3.7 software. Nodes in the network represent active components and target

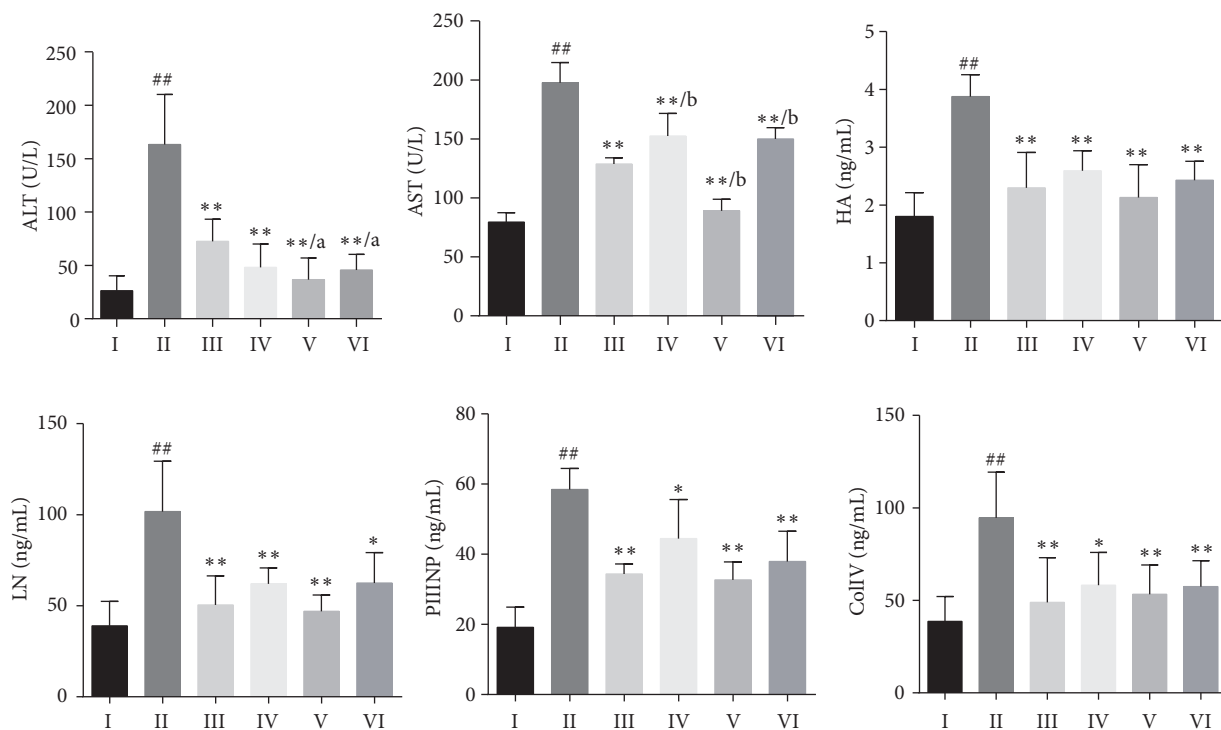


FIGURE 2: Effect of DSLHG on serum biochemical levels in CCl_4 -induced liver fibrosis rats (mean \pm SD). ^{##} $P < 0.01$, compared with the normal control group; $*$ $P < 0.05$, $**P < 0.01$, compared with the model group; ^a $P < 0.05$, ^b $P < 0.01$, compared with the positive control group. I: the normal control group; II: the model group; III: the positive control group; IV: DSLHG high-dose group; V: DSLHG medium-dose group; VI: DSLHG low-dose group.

genes. The edges indicate that the ingredients interact with the targets. The Protein-Protein Interaction (PPI) network of DSLHG on liver fibrosis was constructed using the STRING database (<https://string-db.org/>) combined with the Network Analyzer plugin of Cytoscape to filter out hub genes.

2.8. Pathway and Functional Enrichment Analysis. We carried out Gene Ontology (GO) function analysis and signaling pathway enrichment analysis for predicting targets of DSLHG on liver fibrosis by using DAVID bioinformatics resources 6.8 (<https://david.ncicrf.gov/>).

2.9. Statistical Analysis. All experimental data were taken on the mean \pm standard deviation (SD). Statistical analyses were performed with GraphPad Prism 6.0 statistical software. Rank data were analyzed with the rank sum test. A one-way analysis of variance (ANOVA) test was used to compare the mean of different groups. The data were compared by Student's *t* test between two groups, and $P < 0.05$ was considered as statistically significant.

3. Results

3.1. Animal Experiments. The results of serum biochemical indicators in rats are shown in Figure 2. Compared with the model group, ALT, AST, HA, LN, PIIINP, and Col IV levels in rat serum were significantly reduced in DSLHG groups, as well as in the positive control group ($P < 0.05$ or $P < 0.01$).

HE and Masson staining of liver sections were shown in Supplementary Figure 1. As shown in Figure 3, in normal control group, the hepatic lobule structure was clear, and hepatic cords were arranged radially around the central veins, and only a small amount of blue collagen fiber deposition was observed, while the liver tissue of model group indicated thickened capsule, destroyed or disappearing partial normal hepatic lobular structure, and structurally appearing “pseudolobule.” Compared with model group, the histopathological examination showed that collagen deposition, liver inflammation activity, and liver fibrosis significantly reduced after treatment with DSLHG and silibinin. Additionally, no obvious pseudolobules were observed.

As shown in Table 1, rank sum test showed statistical difference in the pathological and fibrosis changes between all treatment groups and the model group ($P < 0.05$). Unfortunately, none of the DSLHG groups were significantly different from the silibinin group in either of these parameters ($P > 0.05$). These results showed that DSLHG had an obvious anti-liver fibrosis effect.

3.2. Active Ingredients Filtering. Total of 513 chemical constituents of seven individual herbs (Sodium Sulfate was not found in the database) in DSLHG were retrieved from TCMSP, including 61 ingredients in LH, 92 in RR, 62 in PC, 98 in GF, 17 in AF, 106 in AR, and 77 in CR. All compounds were subjected to ADME screening, and a total of 111 active compounds had $\text{OB} \geq 30\%$ and $\text{DL} \geq 0.18$. There are 10 compounds

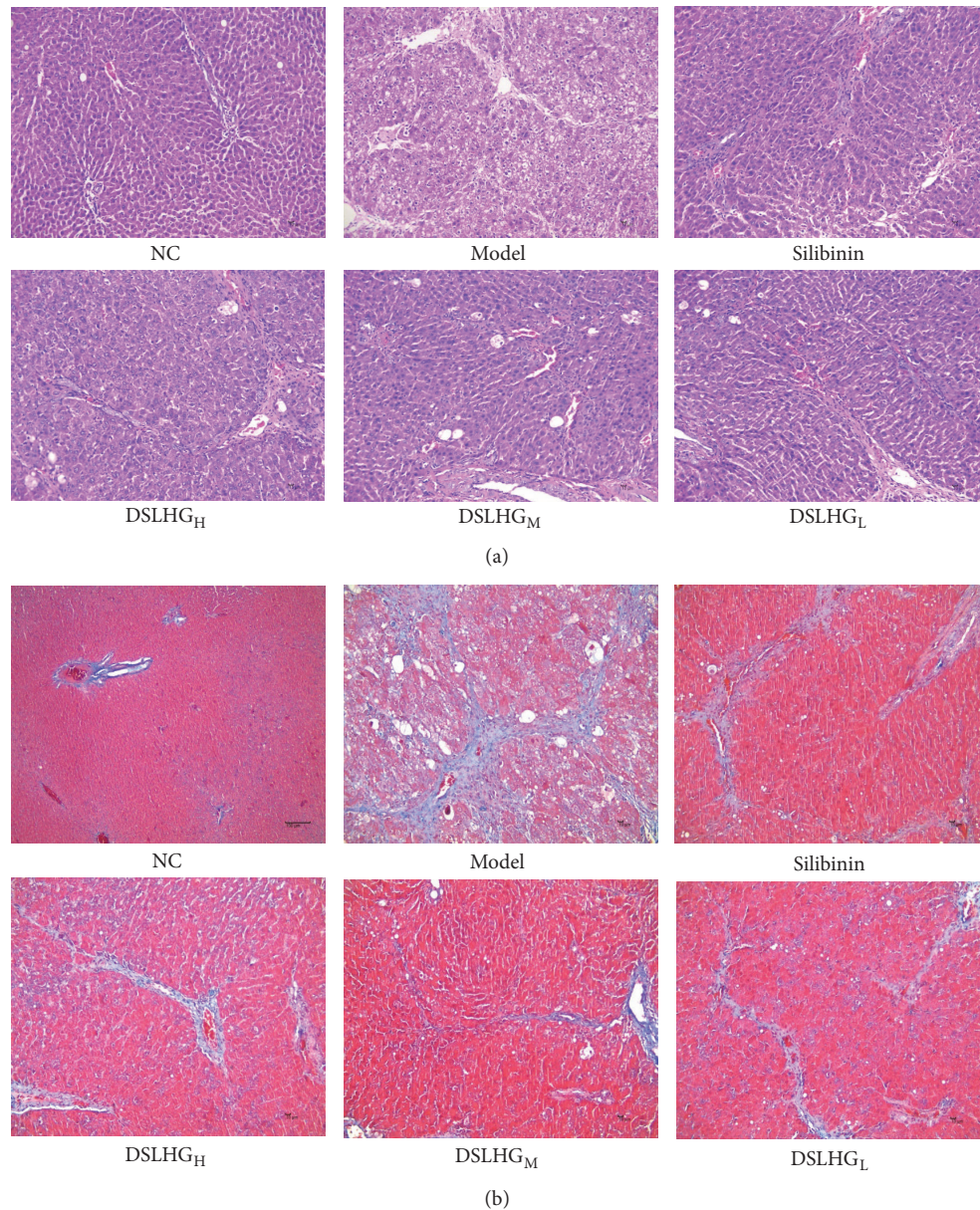


FIGURE 3: Histological results of liver tissues for each group. (a) HE staining ($\times 200$); (b) Masson's trichrome staining ($\times 200$). NC: the normal control group; Model: the model group; Silibinin: the positive control group; DSLHG_H: DSLHG high-dose group; DSLHG_M: DSLHG medium-dose group; DSLHG_L: DSLHG low-dose group.

in LH, 16 compounds in RR, 10 compounds in PC, 15 compounds in GF, 5 compounds in AF, 6 compounds in AR, and 49 compounds in CR, respectively. Due to duplication, fifteen of these compounds were deleted, resulting in 96 effective active ingredients. In addition, among the compounds below the OB and DL screening criteria, 12 (emodin, chrysophanol, physcion [24–26], resveratrol [27], polydatin [28], geniposide, genipin, geniposidic acid, genipin 1-gentiobioside [29–32], dehydrocostus lactone [33], neohesperidin [34], and tetrahydropalmatine [35]) were considered to be biologically active compounds, and their protective effect on liver has

been reported. Therefore, the selected 108 compounds (Supplementary Table 1) from DSLHG formula were subjected to further analysis.

3.3. Potential Targets in DSLHG. Top 10 targets with the highest Fit Score were selected. Total of 192 potential targets were obtained from 108 active ingredients after removing the redundancy (Supplementary Table 2), including MDM2, TNFBRI, MAPK14, and SRC, involved in inflammation, hepatic lipid metabolism, and the development of hepatic fibrosis. In order to make the targets more concentrated, we

TABLE 1: Comparison of histological activity and fibrosis stages.

Groups	N	A				F					
		A0	A1	A2	A3	F0	F1	F2	F3	F4	
Normal	6	2	4	0	0	3	3	0	0	0	
Model	6	0	0	1	5 ^{##}	0	0	0	2	4 ^{##}	
Silibinin	6	0	3	3	0**	0	1	4	1	0**	
DSLHG _H	6	0	2	3	1**	0	0	4	2	0**	
DSLHG _M	6	0	4	2	0**	0	2	3	1	0**	
DSLHG _L	6	0	2	4	0**	0	2	4	0	0**	

A: activity grade, A0-A3; F: fibrosis stage, F0-F4. ^{##} $P < 0.01$, compared with the normal control group; ** $P < 0.01$, compared with the model group.

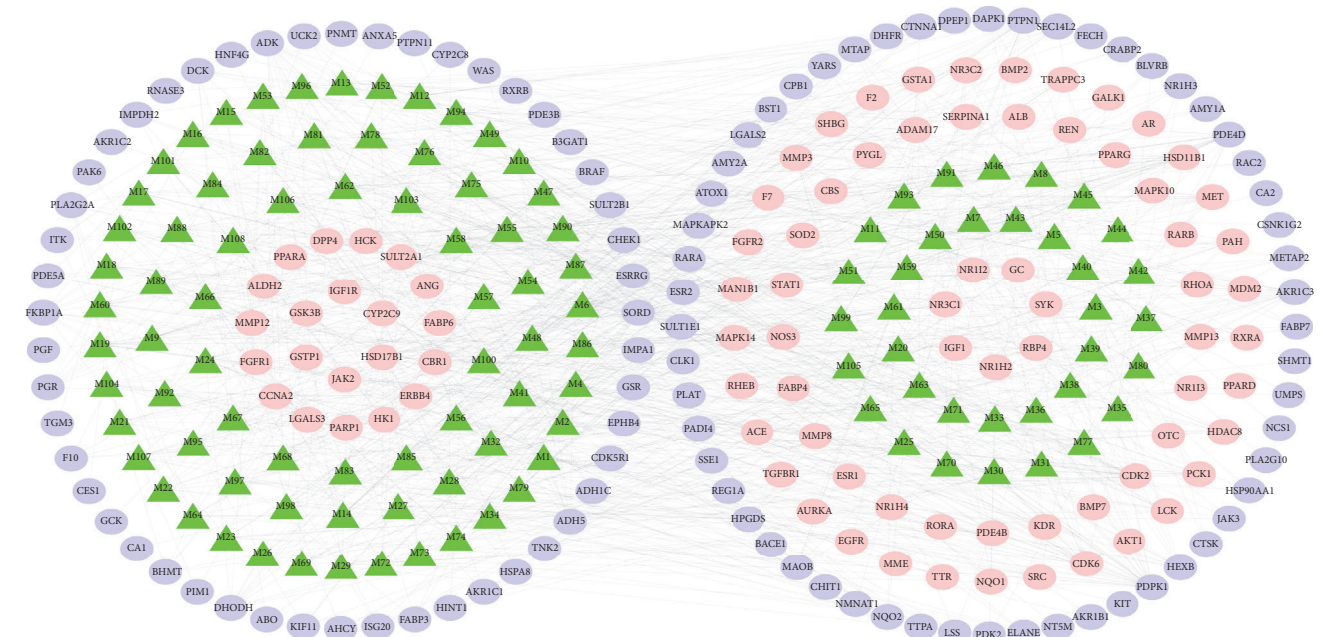


FIGURE 4: Potential active compound-target network of DSLHG acting on liver fibrosis. A compound node and a target node are linked if the protein is targeted by the related compounds. Green triangle nodes represent the active compounds of DSLHG; ellipse and circular nodes are the potential targets of DSLHG; the overlap of the potential targets of the active compounds in DSLHG formula and the liver fibrosis-related targets is indicated with pink circular nodes.

deleted 106 target genes which could not correspond to the disease. As shown in Table 2, 86 of 192 potential targets were associated with liver fibrosis.

3.4. Compounds-Targets (C-T) Network Construction and Analysis. As shown in Figure 4, the 108 active compounds and related 192 target genes constructed the network schematic diagram. Totally, this C-T network is composed of 300 nodes (108 active compounds and 192 potential targets) and 1080 edges. In the picture, the edges indicate an association between the active ingredients and the targets. The degree values indicate the intensity of the interaction between the components and the targets. Green triangle nodes represent the active compounds of DSLHG. Circular nodes represent the potential targets of DSLHG, and the overlaps between the potential targets of the DSLHG and the liver fibrosis-related targets are indicated with pink circular nodes.

According to the network, one target gene may be complicatedly linked to multiple active ingredients of different herbs, which suggest that these compounds might synergistically contribute to the pharmacological effect of the DSLHG in the treatment of hepatic fibrosis. In addition, different active ingredients can also target the same gene, reflecting its multicomponent, multitarget, and antifibrosis effect, that was consistent with the multicomponent and multitarget characteristics of TCM.

3.5. PPI Network Construction and Analysis. 86 target genes associated with active ingredients and liver fibrosis were imported into the STRING database for PPI network construction and analysis. There are 83 interacting targets in the network (HDAC8, RORA, and PDE4B are not involved in protein interaction), resulting in 594 edges representing the interaction between proteins (Figure 5(a)). Then, the PPI network was screened according to the degree values. In this

TABLE 2: The overlapping targets for potential targets of the active compounds in DSLHG formula and the liver fibrosis-related targets.

No.	Protein name	Gene name	UniProt
P1	Angiotensin-converting enzyme	ACE	P12821
P2	Disintegrin and metalloproteinase domain-containing protein 17	ADAM17	P78536
P3	RAC-alpha serine/threonine-protein kinase	AKT1	P31749
P4	Serum albumin	ALB	P02768
P5	Aldehyde dehydrogenase, mitochondrial	ALDH2	P05091
P6	Angiogenin	ANG	P03950
P7	Androgen receptor	AR	P10275
P8	Aurora kinase A	AURKA	O14965
P9	Bone morphogenetic protein 2	BMP2	P12643
P10	Bone morphogenetic protein 7	BMP7	P18075
P11	Carbonyl reductase [NADPH] 1	CBR1	P16152
P12	Cystathionine beta-synthase	CBS	P35520
P13	Cyclin-A2	CCNA2	P20248
P14	Cyclin-dependent kinase 2	CDK2	P24941
P15	Cyclin-dependent kinase 6	CDK6	Q00534
P16	Cytochrome P450 2C9	CYP2C9	P11712
P17	Dipeptidyl peptidase 4	DPP4	P27487
P18	Epidermal growth factor receptor	EGFR	P00533
P19	Receptor tyrosine-protein kinase erbB-4	ERBB4	Q15303
P20	Estrogen receptor	ESR1	P03372
P21	Prothrombin	F2	P00734
P22	Coagulation factor VII	F7	P08709
P23	Fatty acid-binding protein, adipocyte	FABP4	P15090
P24	Gastrotropin	FABP6	P51161
P25	Fibroblast growth factor receptor 1	FGFR1	P11362
P26	Fibroblast growth factor receptor 2	FGFR2	P21802
P27	Galactokinase	GALK1	P51570
P28	Vitamin D-binding protein	GC	P02774
P29	Glycogen synthase kinase-3 beta	GSK3B	P49841
P30	Glutathione S-transferase A1	GSTA1	P08263
P31	Glutathione S-transferase P	GSTP1	P09211
P32	Tyrosine-protein kinase HCK	HCK	P08631
P33	Histone deacetylase 8	HDAC8	Q9BY41
P34	Hexokinase-1	HK1	P19367
P35	Corticosteroid 11-beta-dehydrogenase isozyme 1	HSD11B1	P28845
P36	Estradiol 17-beta-dehydrogenase 1	HSD17B1	P14061
P37	Insulin-like growth factor I	IGF1	P05019
P38	Insulin-like growth factor 1 receptor	IGF1R	P08069
P39	Tyrosine-protein kinase JAK2	JAK2	O60674
P40	Vascular endothelial growth factor receptor 2	KDR	P35968
P41	Tyrosine-protein kinase Lck	LCK	P06239
P42	Galectin-3	LGALS3	P17931
P43	Endoplasmic reticulum mannosyl-oligosaccharide 1,2-alpha-mannosidase	MAN1B1	Q9UKM7
P44	Mitogen-activated protein kinase 10	MAPK10	P53779
P45	Mitogen-activated protein kinase 14	MAPK14	Q16539
P46	E3 ubiquitin-protein ligase Mdm2	MDM2	Q00987
P47	Hepatocyte growth factor receptor	MET	P08581
P48	Nepriylsin	MME	P08473
P49	Macrophage metalloelastase	MMP12	P39900
P50	Collagenase 3	MMP13	P45452
P51	Stromelysin-1	MMP3	P08254
P52	Neutrophil collagenase	MMP8	P22894
P53	Nitric oxide synthase, endothelial	NOS3	P29474

TABLE 2: Continued.

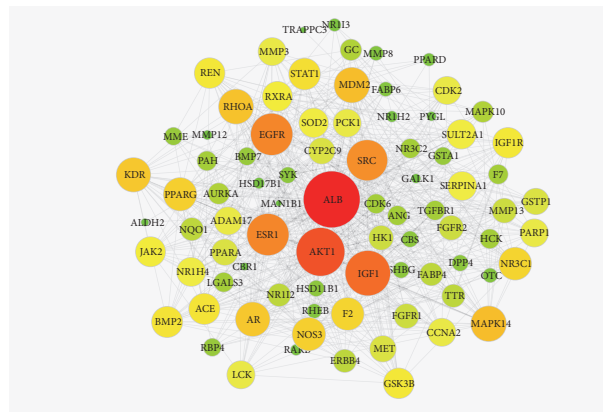
No.	Protein name	Gene name	UniProt
P54	NAD(P)H dehydrogenase [quinone] 1	NQO1	P15559
P55	Oxysterols receptor LXR-beta	NRIH2	P55055
P56	Bile acid receptor	NRIH4	Q96RI1
P57	Nuclear receptor subfamily 1 group 1 member 2	NRII2	O75469
P58	Nuclear receptor subfamily 1 group 1 member 3	NRII3	Q14994
P59	Glucocorticoid receptor	NR3C1	P04150
P60	Mineralocorticoid receptor	NR3C2	P08235
P61	Ornithine carbamoyltransferase, mitochondrial	OTC	P00480
P62	Phenylalanine-4-hydroxylase	PAH	P00439
P63	Poly [ADP-ribose] polymerase 1	PARP1	P09874
P64	Phosphoenolpyruvate carboxykinase, cytosolic [GTP]	PCK1	P35558
P65	cAMP-specific 3',5'-cyclic phosphodiesterase 4B	PDE4B	Q07343
P66	Peroxisome proliferator-activated receptor alpha	PPARA	Q07869
P67	Peroxisome proliferator-activated receptor delta	PPARD	Q03181
P68	Peroxisome proliferator-activated receptor gamma	PPARG	P37231
P69	Glycogen phosphorylase, liver form	PYGL	P06737
P70	Retinoic acid receptor beta	RARB	P10826
P71	Retinol-binding protein 4	RBP4	P02753
P72	Renin	REN	P00797
P73	GTP-binding protein Rheb	RHEB	Q15382
P74	Transforming protein RhoA	RHOA	P61586
P75	Nuclear receptor ROR-alpha	RORA	P35398
P76	Retinoic acid receptor RXR-alpha	RXRA	P19793
P77	Alpha-1-antitrypsin	SERPINA1	P01009
P78	Sex hormone-binding globulin	SHBG	P04278
P79	Superoxide dismutase [Mn], mitochondrial	SOD2	P04179
P80	Proto-oncogene tyrosine-protein kinase Src	SRC	P12931
P81	Signal transducer and activator of transcription 1-alpha/beta	STAT1	P42224
P82	Bile salt sulfotransferase	SULT2A1	Q06520
P83	Tyrosine-protein kinase SYK	SYK	P43405
P84	TGF-beta receptor type-1	TGFBR1	P36897
P85	Trafficking protein particle complex subunit 3	TRAPPC3	O43617
P86	Transthyretin	TTR	P02766

work, the target genes with a degree value greater than 10 were selected as the core genes for further analysis and a total of 47 targets were screened out.

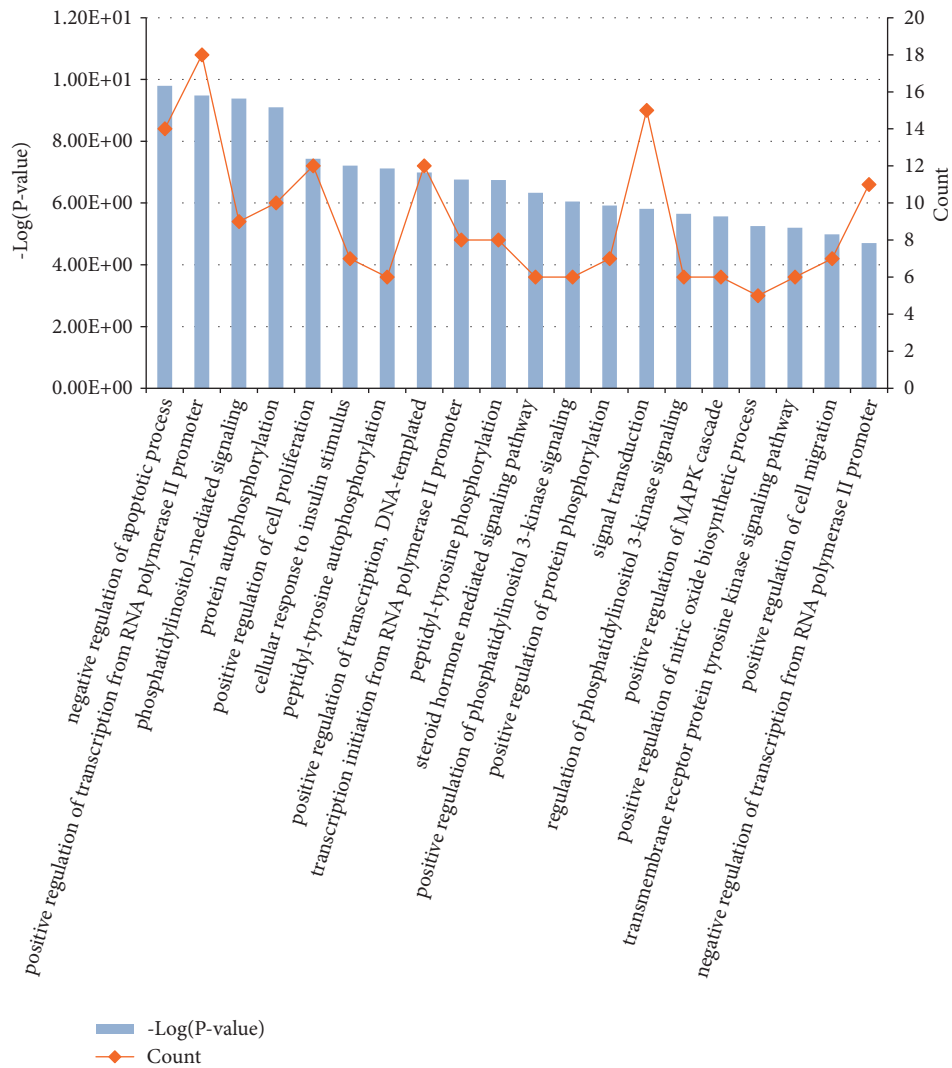
3.6. GO Functional Annotation Analysis. A total of 47 key potential genes that may be involved in liver fibrosis were uploaded to the DAVID panel for analyzing their biological process. The functional distribution of 47 targets was explored by GO functional analysis. The results of GO analysis of the predicted key targets of DSLHG acting on liver fibrosis are shown in Figure 5(b), which listed the 20 GO terms with low P values and more targets enrichment. The results showed that these targets have a strong association with physiological mechanisms, such as signal transduction, protein autophosphorylation, and positive regulation of cell proliferation. These results indicated that DSLHG may play

a key role in antihepatic fibrosis by manipulating these biological processes which lead to the pathogenesis of liver fibrosis.

3.7. Kyoto Encyclopedia of Genes and Genomes (KEGG) Signaling Pathway Analysis. To determine the relevant signaling pathways involved in the anti-liver fibrosis effect of DSLHG, we conducted pathway enrichment analysis using KEGG pathways. A total of 47 targets obtained 60 KEGG signaling pathways, and 47 channels were significantly enriched ($P < 0.05$). The senior bubble map visually showed these significantly enriched pathways (Figure 6). The color and size of the nodes in the bubble graph were decided by the number of associated genes and the P values. The colors from green to red reflected the P values from high to low, and the size of the nodes indicated how many target genes are associated.



(a)



(b)

FIGURE 5: The protein interaction of overlap of the potential targets of the chemical components in DSLHG with the liver fibrosis-related target genes and annotation analysis of core genes. (a) The PPI network of 86 overlap genes. (b) GO function analysis for hub genes. *Notes.* The nodes were overlap protein genes; the size of nodes from small to large represent the degree value from low to high; and these nodes color changes from green to red to indicate that the degree values change from low to high.

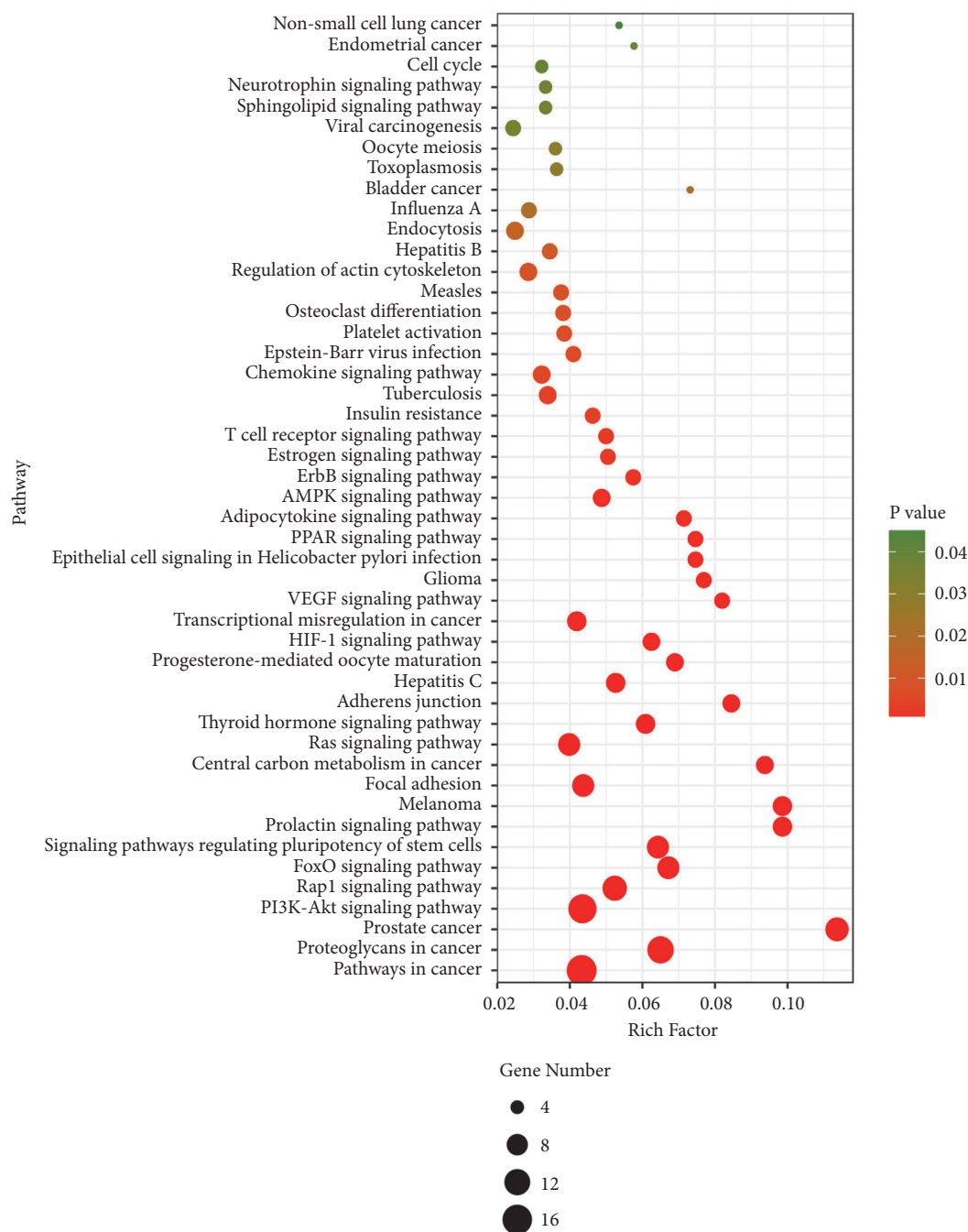


FIGURE 6: KEGG pathway enrichment analysis for core targets of DSLHG acting on liver fibrosis.

The results of KEGG pathways enrichment analysis indicated the multiple channels and mechanisms of action of DSLHG against liver fibrosis.

The top 10 pathways with lower P values and more genes enrichment are listed in Table 3, including PI3K-Akt signaling pathway, AMPK signaling pathway, Ras signaling pathway, T cell receptor signaling pathway, PPAR signaling pathway, VEGF signaling pathway, and FoxO signaling pathway being enriched. These signaling pathways involve inflammation, metabolism, and ECM deposition. Taken together, these signaling pathways seem to be closely related to the beneficial

effects of DSLHG against liver fibrosis. The illustrated network that contains main chemicals-targets-signaling pathway of DSLHG was established to understand their interaction (Figure 7).

4. Discussion

Hepatic fibrosis is considered as the wound healing in response to the chronic liver damage caused by various factors. Excessive production and abnormal deposition of ECM are caused by the complicated interaction between

TABLE 3: The important signaling pathways of core target genes.

Pathway ID	Term	Target genes	P-Value
hsa04151	PI3K-Akt signaling pathway	AKT1, EGFR, FGFR1, FGFR2, RXRA, MET, IGF1, CDK2, KDR, PCK1, IGF1R, GSK3B, MDM2, NOS3, JAK2	7.21E-0.9
hsa04068	FoxO signaling pathway	AKT1, EGFR, IGF1R, MAPK14, MDM2, IGF1, CDK2, PCK1, SOD2	1.14E-06
hsa04014	Ras signaling pathway	AKT1, EGFR, IGF1R, FGFR1, FGFR2, MET, RHOA, IGF1, KDR	5.39E-05
hsa04919	Thyroid hormone signaling pathway	AKT1, RXRA, GSK3B, ESRI, MDM2, STAT1, SRC	6.15E-05
hsa04015	Rap1 signaling pathway	AKT1, EGFR, FGFR2, IGF1R, FGFR1, MAPK14, MET, RHOA, IGF1, SRC, KDR	3.55E-07
hsa04510	Focal adhesion	AKT1, EGFR, IGF1R, GSK3B, MET, RHOA, IGF1, SRC, KDR	2.77E-05
hsa05205	Proteoglycans in cancer	AKT1, EGFR, IGF1R, FGFR1, ERBB4, MAPK14, MET, RHOA, ESRI, MDM2, IGF1, SRC, KDR	1.35E-09
hsa05200	Pathways in cancer	AKT1, EGFR, FGFR2, FGFR1, AR, BMP2, RXRA, MET, PPARG, IGF1, STAT1, CDK2, IGF1R, GSK3B, RHOA, MDM2, GSTP1	4.03E-10
hsa05215	Prostate cancer	AKT1, FGFR2, EGFR, IGF1R, FGFR1, AR, GSK3B, MDM2, IGF1, CDK2	1.91E-09
hsa04066	HIF-1 signaling pathway	AKT1, EGFR, IGF1R, IGF1, HK1, NOS3	2.70E-04

various types of cells and cytokines in the liver, characterized by imbalance between the degradation and synthesis of ECM, resulting in a series of changes during the initiation and progression of liver fibrosis [3, 36, 37]. The occurrence of liver fibrosis is often accompanied by a certain degree of inflammatory response. Inflammation is one of the most typical features of viral, alcoholic, fatty, and autoimmune chronic liver disease. For a long time, many scholars have been working to explore the certain role of inflammation in the pathogenesis of liver fibrosis, such as the role of inflammatory mediators in the hepatic stellate cells (HSCs) activation and development of liver fibrosis [38]. HSCs are the main cells responsible for synthesis of ECM in normal and fibrotic liver and play central role in the development of liver fibrosis [39–41]. Once HSCs are activated through paracrine and autocrine routes, the imbalance between ECM synthesis and degradation was interfered, which results in aberrant accumulation of ECM in the liver [42, 43].

FoxO, a key downstream regulator in the PI3K-Akt signaling pathway belonging to subclass of the forkhead proteins family, regulates metabolic homeostasis in response to oxidative stress. Moreover, oxidative stress resistance, apoptosis, and glucose metabolism were also modulated by FoxO [44]. Importantly, FoxO transcription factors benefit liver fibrosis through inhibiting proliferation and transdifferentiation of HSCs [45].

As the downstream factor of the PI3K-Akt signaling pathway, FoxOs are controlled by Akt (protein kinase B, PKB). The PI3K/Akt signaling pathway is one of the important signaling pathways, which has increasingly raised concern under various diseases context. The PI3K-Akt signaling pathway can be activated by many types of cellular stimuli or toxic insults and regulates fundamental cellular functions, such as transcription, translation, proliferation, growth, and survival [46]. Some researchers [47, 48] have reported that PI3K and

Akt are important in the process of the activation of hepatic stellate cells (HSCs), cell proliferation, and collagen synthesis. In contrast, PI3K and Akt are also involved in the regulation of HSCs apoptosis, which may be one of the important pathways delaying the development of liver fibrosis.

At present, most of the western medicines used for the treatment of liver fibrosis are effective only under a certain condition, with difficulty in achieving multitarget and multichelon coverage. However, most diseases are associated with multiple targets; thus, it is difficult to achieve appropriate therapeutic results against a single target. The pharmacodynamic mechanisms of TCM against liver fibrosis have multiple levels and multiple targets and pay attention to the characteristics of overall regulation [10]. A new approach that analyzes TCM with network pharmacology may be a reliable way to overcome disease [49]. Cumulating data have shown that network pharmacology can reveal the interactions between multiple targets of compounds present in Chinese herbal medicines [50].

In this study, through the analysis of DSLHG compound-target-pathway network, we found that the main active components of DSLHG could act on multiple targets, indicating the multicomponent, multitarget, and overall regulation of formula. In addition, DSLHG generates the anti-liver fibrosis effect by acting on multiple pathways, multiple targets, and multiple biological processes. The predicted targets and signaling pathways in this study provide ideas for experiments to verify the key target proteins and mechanisms of antifibrosis of DSLHG in the future.

5. Conclusion

In summary, this study used a network pharmacology approach to construct a biological network to display the interactions between compounds and protein/gene targets

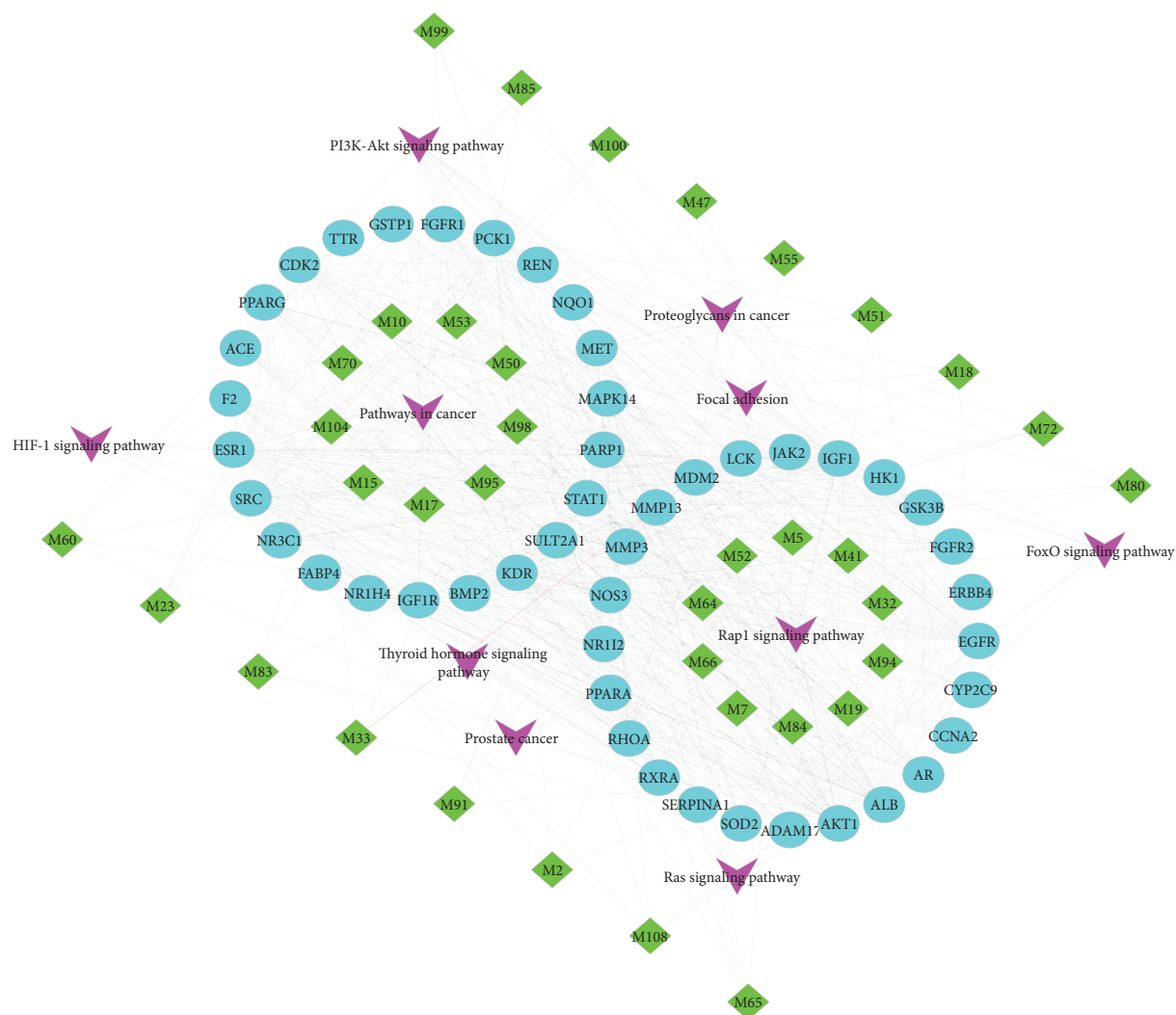


FIGURE 7: Main active compound (degree>3) core target-pathway network of DSLHG on treating liver fibrosis. Core target genes are shown with blue circular nodes; green diamond nodes represent the active compounds in DSLHG formula and purple V nodes are signaling pathways.

at a molecular or systemic level. The results indicate that DSLHG can achieve antifibrosis by acting on multiple targets and multiple pathways. Through our network analysis and prediction, the mechanisms of DSLHG formula at the molecular level are clarified, which might provide new ideas for developing new drug treatment or novel therapeutical strategies for liver fibrosis. Next, we will verify the results of network analysis prediction through manipulating the targeted molecular via pharmacological or genetical methods.

Data Availability

The data used to support the findings of this study are included within the article and the supplementary information files.

Disclosure

Yueying Tao and Kunming Tian are co-first authors, and Zehui Chen and Yingbiao Tian are joint corresponding authors.

Conflicts of Interest

There are no conflicts of interest to declare.

Authors' Contributions

Yongai Xiong, Zehui Chen, and Yingbiao Tian proposed the idea and designed the study. Yueying Tao and Kunming Tian performed the study. Ji Chen, Danfeng Tan, and Yan Liu participated in 'in silico' analysis and data analysis. Yueying

Tao and Kunming Tian wrote and improved the manuscript. All authors read and approved the final manuscript. Yueying Tao and Kunming Tian contributed equally to this work.

Acknowledgments

This study was supported by the project which named 8 kinds of hospital preparations and clinical research such as Fuke Qingre Zhidai granules [No. 20153028]. And the project was approved by the Science and Technology Department of Guizhou Province, China.

Supplementary Materials

Supplementary 1. Supplementary Table 1: the information of active compounds in DSLHG formula. *Supplementary 2.* Supplementary Table 2: the 192 potential targets of active ingredients in DSLHG formula. *Supplementary 3.* Supplementary Figure 1: HE and Masson staining of liver sections for each group. (*Supplementary Materials*)

References

- [1] U. E. Lee and S. L. Friedman, "Mechanisms of hepatic fibrogenesis," *Best Practice & Research: Clinical Gastroenterology*, vol. 25, no. 2, pp. 195–206, 2011.
- [2] E. Novo, S. Cannito, C. Paternostro, C. Bocca, A. Miglietta, and M. Parola, "Cellular and molecular mechanisms in liver fibrogenesis," *Archives of Biochemistry and Biophysics*, vol. 548, pp. 20–37, 2014.
- [3] D. Li, W. Li, Y. Chen et al., "Anti-fibrotic role and mechanism of *Periplaneta americana* extracts in CCl₄-induced hepatic fibrosis in rats," *Acta Biochimica et Biophysica Sinica*, vol. 50, no. 5, pp. 491–498, 2018.
- [4] Y. S. Chiu, C. Wei, Y. Lin, Y. Hsu, and M. Chang, "IL-20 and IL-20R1 antibodies protect against liver fibrosis," *Hepatology*, vol. 60, no. 3, pp. 1003–1014, 2014.
- [5] T. R. Harris, S. Kodani, J. Yang et al., "An ω -3-enriched diet alone does not attenuate CCl₄-induced hepatic fibrosis," *The Journal of Nutritional Biochemistry*, vol. 38, pp. 93–101, 2016.
- [6] Y. Guo, X. Liang, M. Meng et al., "Hepatoprotective effects of Yulangsang flavone against carbon tetrachloride (CCl₄)-induced hepatic fibrosis in rats," *Phytomedicine*, vol. 33, pp. 28–35, 2017.
- [7] E. Seki and D. A. Brenner, "Recent advancement of molecular mechanisms of liver fibrosis," *Journal of Hepato-Biliary-Pancreatic Sciences*, vol. 22, no. 7, pp. 512–518, 2015.
- [8] H. M. Atta, "Reversibility and heritability of liver fibrosis: Implications for research and therapy," *World Journal of Gastroenterology*, vol. 21, no. 17, pp. 5138–5148, 2015.
- [9] D. Liu and X. B. Jia, "Analysis and discussion about current development of relevant studies on "traditional Chinese medicine components"," *Zhongguo Zhong Yao Za Zhi*, vol. 39, no. 2, pp. 171–174, 2014.
- [10] S. Li and B. Zhang, "Traditional Chinese medicine network pharmacology: theory, methodology and application," *Chinese Journal of Natural Medicines*, vol. 11, no. 2, pp. 110–120, 2013.
- [11] F. Liu, X. Du, P. Liu, Y. Sun, and Y. Zhang, "Screening and analysis of key active constituents in Guanxinshutong capsule using mass spectrum and integrative network pharmacology," *Chinese Journal of Natural Medicines*, vol. 16, no. 4, pp. 302–312, 2018.
- [12] J. Fang, L. Wang, T. Wu et al., "Network pharmacology-based study on the mechanism of action for herbal medicines in Alzheimer treatment," *Journal of Ethnopharmacology*, vol. 196, pp. 281–292, 2017.
- [13] M. X. Dong, Y. Jia, Y. B. Zhang et al., "Emodin protects rat liver from CCl₄-induced fibrogenesis via inhibition of hepatic stellate cells activation," *World Journal of Gastroenterology*, vol. 15, no. 38, pp. 4753–4762, 2009.
- [14] X. Wang, C. Niu, X. Zhang et al., "Emodin suppresses activation of hepatic stellate cells through p38 mitogen-activated protein kinase and Smad signaling pathways in vitro," *Phytotherapy Research*, vol. 32, no. 12, pp. 1–11, 2018.
- [15] Y. Zhan, D. Li, H. Wei et al., "Emodin on hepatic fibrosis in rats," *Chinese Medical Journal*, vol. 113, no. 7, pp. 599–601, 2000.
- [16] M. Z. Guo, X. S. Li, H. R. Xu et al., "Rhein inhibits liver fibrosis induced by carbon tetrachloride in rats," *Acta Pharmacologica Sinica*, vol. 23, no. 8, pp. 739–744, 2002.
- [17] Y. Jiao, Y. Wu, and D. Du, "Polydatin inhibits cell proliferation, invasion and migration, and induces cell apoptosis in hepatocellular carcinoma," *Brazilian Journal of Medical and Biological Research*, vol. 51, no. 4, Article ID e6867, 2018.
- [18] X. Zhao, R. Li, Y. Liu et al., "Polydatin protects against carbon tetrachloride-induced liver fibrosis in mice," *Archives of Biochemistry and Biophysics*, vol. 629, pp. 1–7, 2017.
- [19] J. Ru, P. Li, J. Wang et al., "TCMSP: a database of systems pharmacology for drug discovery from herbal medicines," *Journal of Cheminformatics*, vol. 6, no. 1, p. 13, 2014.
- [20] A. Y. Lee, W. Park, T. Kang, M. H. Cha, and J. M. Chun, "Network pharmacology-based prediction of active compounds and molecular targets in Yijin-Tang acting on hyperlipidaemia and atherosclerosis," *Journal of Ethnopharmacology*, vol. 221, pp. 151–159, 2018.
- [21] X. Wang, Y. Shen, S. Wang et al., "PharmMapper 2017 update: A web server for potential drug target identification with a comprehensive target pharmacophore database," *Nucleic Acids Research*, vol. 45, no. 1, pp. W356–W360, 2017.
- [22] G. Stelzer, R. Rosen, I. Plaschkes et al., "The GeneCards suite: from gene data mining to disease genome sequence analysis," *Current Protocols in Bioinformatics*, vol. 54, pp. 1.30.1–1.30.33, 2016.
- [23] A. Hamosh, A. F. Scott, J. S. Amberger, C. A. Bocchini, and V. A. McKusick, "Online Mendelian Inheritance in Man (OMIM), a knowledgebase of human genes and genetic disorders," *Nucleic Acids Research*, vol. 33, pp. D514–D517, 2005.
- [24] L. Feng, J. Zhang, J. Qian, W. Gang, and M. Zhenyu, "Emodin alleviates CCl₄-induced liver fibrosis by suppressing epithelial-mesenchymal transition and transforming growth factor- β 1 in rats," *Molecular Medicine Reports*, vol. 18, no. 3, pp. 3262–3270, 2018.
- [25] Y. Lian, X. Xia, H. Zhao, and Y. Zhu, "The potential of chrysothanol in protecting against high fat-induced cardiac injury through Nrf2-regulated anti-inflammation, anti-oxidant and anti-fibrosis in Nrf2 knockout mice," *Biomedicine & Pharmacotherapy*, vol. 93, pp. 1175–1189, 2017.
- [26] Y. L. Lin, C. F. Wu, and Y. T. Huang, "Phenols from the roots of *Rheum palmatum* attenuate chemotaxis in rat hepatic stellate cells," *Planta Medica*, vol. 74, no. 10, pp. 1246–1252, 2008.
- [27] S. B. Abdu and F. M. Al-Bogami, "Influence of resveratrol on liver fibrosis induced by dimethylnitrosamine in male rats," *Saudi Journal of Biological Sciences*, vol. 26, no. 1, pp. 201–209, 2019.

- [28] R. Li, J. Li, Y. Huang et al., "Polydatin attenuates diet-induced nonalcoholic steatohepatitis and fibrosis in mice," *International Journal of Biological Sciences*, vol. 14, no. 11, pp. 1411–1425, 2018.
- [29] M. Inao, S. Mochida, A. Matsui et al., "Japanese herbal medicine Inchin-ko-to as a therapeutic drug for liver fibrosis," *Journal of Hepatology*, vol. 41, no. 4, pp. 584–591, 2004.
- [30] A. Kitano, S. Saika, O. Yamanaka et al., "Genipin suppresses subconjunctival fibroblast migration, proliferation and myofibroblast transdifferentiation," *Ophthalmic Research*, vol. 38, no. 6, pp. 355–360, 2006.
- [31] S. J. Kim, K. M. Kim, J. Park, J. H. Kwak, Y. S. Kim, and S. M. Lee, "Geniposidic acid protects against D-galactosamine and lipopolysaccharide-induced hepatic failure in mice," *Journal of Ethnopharmacology*, vol. 146, no. 1, pp. 271–277, 2013.
- [32] T. Zhou, W. Zhao, G. Fan, Y. Chai, and Y. Wu, "Isolation and purification of iridoid glycosides from *Gardenia jasminoides* Ellis by isocratic reversed-phase two-dimensional preparative high-performance liquid chromatography with column switch technology," *Journal of Chromatography B*, vol. 858, no. 1–2, pp. 296–301, 2007.
- [33] J. Mao, M. Yi, R. Wang et al., "Protective effects of costunolide against d-galactosamine and lipopolysaccharide-induced acute liver injury in mice," *Frontiers in Pharmacology*, vol. 9, p. 1469, 2018.
- [34] N. Miceli, M. R. Mondello, M. T. Monforte et al., "Hypolipidemic effects of citrus bergamia risso et poiteau juice in rats fed a hypercholesterolemic diet," *Journal of Agricultural and Food Chemistry*, vol. 55, no. 26, pp. 10671–10677, 2007.
- [35] C. Sun, Z. Chen, H. Wang, and K. Ding, "Tetrahydropalmatine prevents high-fat diet-induced hyperlipidemia in golden hamsters (*Mesocricetus auratus*)," *Medical Science Monitor*, vol. 24, pp. 6564–6572, 2018.
- [36] J. Ding, J. Yu, C. Wang et al., "Ginkgo biloba extract alleviates liver fibrosis induced by CCl_4 in rats," *Liver International*, vol. 25, no. 6, pp. 1224–1232, 2005.
- [37] B. Gao and R. Bataller, "Alcoholic liver disease: pathogenesis and new therapeutic targets," *Gastroenterology*, vol. 141, no. 5, pp. 1572–1585, 2011.
- [38] E. Seki and R. F. Schwabe, "Hepatic inflammation and fibrosis: functional links and key pathways," *Hepatology*, vol. 61, no. 3, pp. 1066–1079, 2014.
- [39] X. Jiang, E. Tsitsiou, S. E. Herrick, and M. A. Lindsay, "MicroRNAs and the regulation of fibrosis," *FEBS Journal*, vol. 277, no. 9, pp. 2015–2021, 2010.
- [40] X. P. Jiang, W. B. Ai, L. Y. Wan et al., "The roles of microRNA families in hepatic fibrosis," *Cell & Bioscience*, vol. 7, no. 1, pp. 34–42, 2017.
- [41] T. Higashi, S. L. Friedman, and Y. Hoshida, "Hepatic stellate cells as key target in liver fibrosis," *Advanced Drug Delivery Reviews*, vol. 121, pp. 27–42, 2017.
- [42] J. P. Li, Y. Gao, S. F. Chu et al., "Nrf2 pathway activation contributes to anti-fibrosis effects of ginsenoside Rg1 in a rat model of alcohol and CCl_4 -induced hepatic fibrosis," *Acta Pharmacologica Sinica*, vol. 35, no. 8, pp. 1031–1044, 2014.
- [43] F. Tacke and R. Weiskirchen, "Update on hepatic stellate cells: pathogenic role in liver fibrosis and novel isolation techniques," *Expert Review of Gastroenterology & Hepatology*, vol. 6, no. 1, pp. 67–80, 2012.
- [44] X. C. Dong, "FOXO transcription factors in non-alcoholic fatty liver disease," *Liver Research*, vol. 1, no. 3, pp. 168–173, 2017.
- [45] M. Adachi, Y. Osawa, H. Uchinami, T. Kitamura, D. Accili, and D. A. Brenner, "The forkhead transcription factor FoxO1 regulates proliferation and transdifferentiation of hepatic stellate cells," *Gastroenterology*, vol. 132, no. 4, pp. 1434–1446, 2007.
- [46] A. M. Martelli, M. Nyäkern, G. Tabellini et al., "Phosphoinositide 3-kinase/Akt signaling pathway and its therapeutical implications for human acute myeloid leukemia," *Leukemia*, vol. 20, no. 6, pp. 911–928, 2006.
- [47] Y. Xiao, J. Wang, Y. Chen et al., "Up-regulation of miR-200b in biliary atresia patients accelerates proliferation and migration of hepatic stellate cells by activating PI3K/Akt signaling," *Cellular Signalling*, vol. 26, no. 5, pp. 925–932, 2014.
- [48] A. Li, J. Wang, M. Wu, X. Zhang, and H. Zhang, "The inhibition of activated hepatic stellate cells proliferation by arctigenin through G_0/G_1 phase cell cycle arrest: persistent p27^{Kip1} induction by interfering with PI3K/Akt/FOXO3a signaling pathway," *European Journal of Pharmacology*, vol. 747, pp. 71–87, 2015.
- [49] W. Dai, H. Chen, and C. Y. Chen, "A network pharmacology-based approach to investigate the novel TCM formula against huntington's disease and validated by support vector machine model," *Evidence-Based Complementary and Alternative Medicine*, vol. 2018, Article ID 6020197, 29 pages, 2018.
- [50] S. Yue, J. Liu, W. Feng et al., "System pharmacology-based dissection of the synergistic mechanism of huangqi and huanglian for diabetes mellitus," *Frontiers in Pharmacology*, vol. 8, article no. 694, 2017.